Vietnam Journal of Science and Technology ***61*** *(2) (2023) 137-164*

doi:10.15625/2525-2518/18032

Electromagnetic heating using nanomaterials and various potential applications

Nguyen Xuan Phuc*, Do Hung Manh, Pham Hong Nam

Institute of Materials Science, Vietnam Academy of Science and Technology, 18 Hoang Quoc Viet, Cau Giay, Ha Noi, Viet Nam

*Email: *phucnx@ims.vast.ac.vn*

Received: 16 January 2023; Accepted for publication: 5 March 2023

Abstract. Electromagnetic heating (EMH) is a process of adsorbing electromagnetic wave energy by a material and converting it into heat. Nanomaterials can serve as novel susceptors in EMH due to the fine size that made them become heat sources from inside, as well as because of new heating mechanisms such as Neel relaxation by magnetic nanoparticles (MNPs) and localized surface plasmon resonance by metallic nanostructures. This review firstly introduces general theoretical & experimental aspects of the alternating electric field (AEF)- and magnetic field (AMF)-stimulated heating. Next, attempts to fabricate MNPs and photothermal nanoparticles (PNPs) of improved heating efficiencies have been reviewed and those with the highest specific loss power have been summarized. Finally, potential applications, including cancer treatment using AMF@MNP hyperthermia and AEF@PNP hyperthermia, AMF@MNP- and AEF@PNP- triggered drug release, as well as nanocomposite processing were particularly highlighted. Besides, other exotic applications such as toxic solvent desorption from adsorbent materials, thermophoresis in precise membrane melting as well as optical signal processing in heat-assisted magnetic memory technology were also outlined. The various applications were attempted to represent into 2 groups: biomedicine, and materials processing; which are composed of localized/targeted and volumetric heating type.

Keywords: electro-magnetic heating, nanoparticles, cancer hyperthermia, nanocomposite processing, nanoscale temperature gradient.

Classification numbers: 2.2.1, 2.4.1, 2.4.3, 2.5.1, 2.9.4.

1. INTRODUCTION

Heating technology has been applied since long time, in both material and component processing, as well as medical treatment [1-4]. Among several advanced heating technologies developed (such as resistive heating, vibrational heating, ultrasonic heating, etc.) electromagnetic heating (EMH) is the most studied and widely applied, especially because it is a rapid, controlled, and targeted heating technique. While popular concept identifies an EMH with induction heating, it nowadays can be described as any process of adsorbing an EM wave by a material and converting it into heat. The frequency range of concerns is therefore very wide, covering radio frequency (RF) range, microwave (MW) range, infrared (IF), ultraviolet (UV)

range, etc. [2]. The electromagnetic (EM) energy source used is normally designed to provide alternatively alternating electric field (AEF) or magnetic field (AMF). Efficiency of heating created by EM irradiating subject on a heated object depends much on the susceptibility of the targeted material, which in many cases is a mixture of the matter to-be-heated and assisting component, that exhibits suitable physical property to absorb the energy of the irradiating EM wave. Such an assisting matter is called a susceptor, a heat mediator or heating agent. A well-known example of an electric susceptor is water contained in food to be warmed by household microwave.

During the past three decades, researchers in nanotechnology have discovered many types of nanomaterials that can be used as susceptors for transformation of EM energy to heat [5-7]. The routes for their syntheses as well as the mechanisms of heat generation have been recently reviewed in several papers [6-11]. In many review papers, the nanomaterials for heating susceptor include not only spherical nanoparticles (NPs), but also those of other shape, such as nanofibre, nanotube, nanostar, etc., which exhibit even more interesting heating behaviour [8, 11]. The nanomaterial-mediated heating disposes several advantages over traditional bulk susceptor heating, which is the reason why they have been researched extensively for a wide range of applications. Most attractive application is undoubtedly hyperthermia for cancer treatments, which is the topic of huge number of reports including recent review papers [see e.g. 9, 11, 12]. The applications of nanoparticle-assisted heating are, in fact, much broader. Beyond cancer hyperthermia, they can be used in other branches of biomedicine [10, 13, 14], and in other disciplines including composite thermo-engineering [4, 13] as well as signal control in thermomagnetic memory device [15], or others domains like desorption, catalysis, etc.

The aims of this review paper is to provide a general consideration of the role of magnetic and electric susceptibility of nanomaterials in the heat power generation. The nanomaterials will be classified into two basic classes: magnetic and electric susceptors. After reviewing applications of magnetic nanoparticles (MNPs) and plasmonic nanoparticles (PNPs) in cancer hyperthermia, other various applications will also be reviewed. Discussions on the advantages like targeting, remote controlling, energy saving or single element controlling in particular application will be done.

2. ELECTROMAGNETIC HEATING: THEORETICAL AND EXPERIMENTAL CHARACTERISTICS

2.1. Theoretical characteristics

Distribution of an electromagnetic field in a material is governed by Maxwell equations [1]:

$$\vec{\nabla} \times \vec{\boldsymbol{E}} = -\frac{\partial \vec{\boldsymbol{B}}}{\partial t} \quad (1a)$$

$$\vec{\nabla} \times \vec{\boldsymbol{H}} = \vec{J} + \frac{\partial \vec{\boldsymbol{D}}}{\partial t} \quad (1b)$$

$$\vec{\nabla} \cdot \vec{\boldsymbol{D}} = \rho \quad (1c)$$

$$\vec{\nabla} \cdot \vec{\boldsymbol{B}} = 0 \quad (1d)$$

where **E** is the electric field, **H** is the magnetic field, **D** is the electric displacement, **B** is magnetic induction, **J** is the current density and ρ is the charge density. D and P are related to the material dielectric polarization (P) and magnetization (M) as:

$$D = \varepsilon_o(E + P) = \varepsilon_o(1 + \chi_e).E \quad (2a)$$

$$B = \mu_o(H + M) = \mu_o(1 + \chi_m).H, \quad (2b)$$

χ_e is the material electric susceptibility, and χ_m is magnetic susceptibility.

$$\varepsilon(\omega) = \varepsilon'(\omega) + i\varepsilon''(\omega) = 1 + \chi_e(\omega) \quad (2c)$$

$$\mu(\omega) = \mu'(\omega) + i\mu''(\omega) = 1 + \chi_m(\omega) \quad (2d)$$

are, respectively, electric and magnetic permittivity; ε_o and μ_o are correspondingly electric and magnetic permittivity of vacuum, χ_e and χ_m are correspondingly electric and magnetic susceptibility. The 'prime' and 'double prime' denote the real and imaginary part of the corresponding quantity. ω is the angular frequency, which is related to the field frequency f as $f = \omega/2\pi$. According to the techniques to create the electromagnetic field, the waves are classified into different ranges, including: RF (f = 3 Hz – 300 MHz), MW (f = 300 MHz – 300 GHz), IF (300 GHz-30 THz), visible & near UV (300 THz-3PHz), etc. Electromagnetic heating is based on an adsorption of EM energy from the irradiating field by a material and its dissipation to transform into heat. The heating mechanism depends first of all on the specific response of the material responding to the applied field. For the standard induction heating, a metallic specimen when exposed to a magnetic RF field induces an eddy current to flow roundly on the specimen surface, causing the Joule resistive heating. The food warming by a household microwave, on the other hand, beneficiates the dissipation phenomenon of reorientation polarization of water dipole, whose imaginary parameter $\varepsilon''(\omega)$ becomes almost maximized at the used electric field frequency (2.45 GHz).

The researches on nanomaterials have revealed several new heating mechanisms for the response of nanostructures to EM field. In the next part of this section we will briefly deal with 3 cases (Tab. 1): (a) MNPs in RF magnetic field (H_{rf}), (b) Metallic nanoparticles or PNPs irradiated by light (E_{ph}), (c) carbon nanostructures (CNPs) composite in RF electric field (E_{rf}).

The heating of magnetic fluid by AMF was first theoretically studied by Rosensweig [16], and later on reconsidered and reported in a few other papers [17 - 20]. For superparamagnetic NPs of spherical shape with small diameter when exposed to magnetic field **H**, within the linear response theory (LRT), the differential internal energy (d**U**) and cyclic internal energy (ΔU), are:

$$d\,\boldsymbol{U} = \boldsymbol{H}.d\boldsymbol{B} \quad (3a)$$

$$\Delta U = -\mu_o \oint M.dH \quad (3b)$$

to lag the alternating field ($H = H_0 cos(\omega t) = Re[H_0\, exp(i\omega t)]$), the magnetization is written as $M(t) = Re(\chi H_o \exp(i\omega t))$, which results in

$$\Delta U = 2\,\mu_o H_o^2\,\chi'' \int_0^{2\pi/\omega} sin^2\omega t.dt$$

The volumetric power loss, indicating the conversion of alternating magnetic work to heat is:

$$P = f.\Delta U = \mu_o\,\pi\chi''f\,H_o^2 \quad (4)$$

The ferrofluid of superparamagnetic NPs under irradiation of oscillatory field undergoes simultaneously two types of relaxation motions: Neel relaxation of magnetic moment characterized by relaxation time τ_N, and Brown relaxation of the whole particle mass, characterized by τ_B, which can be described by one effective relaxation time:

$$\tau_{eff} = \frac{\tau_N\tau_B}{\tau_N+\tau_B} \quad (5)$$

The Neel and Brown relaxation times are related to the materials parameters as follows,

$$\tau_N = \tau_0 exp(\frac{K_{eff}\,V_m}{k_B\,T}) \quad (6a)$$

$$\tau_B = \frac{3\,\eta\,V_h}{k_B\,T} \tag{6b}$$

where: τ_0 is a factor equal to 10^{-9}s; V_m, V_h are respectively magnetic particle volume and hydrodynamic (whole) particle volume; K_{eff} is the effective anisotropy, and k_B is the Boltzmann constant. These relaxations of the magnetic nanofluid are related to the energy loss power P via the Debye type formula of imaginary magnetic susceptibility χ'' as follows:

$$\chi'' = \chi_0 \frac{\omega\tau_{eff}}{1+(\omega\tau_{eff})^2} \tag{7}$$

from (4) and (7) one can see that the dissipation energy is proportional to the product of frequency and squared field amplitude, which gets maximum when the frequency $f \approx 1/2\pi.\tau_{eff}$ (i.e. $\omega\tau_{eff} = 1$). Experimental researches for MNPs fluids of various compositions showed that the suitable frequencies for getting high efficiency of heat generation are in the radiofrequency range.

The heating of metallic NPs under irradiation of light. Light-induced heating takes place in different PNPs, which can basically be categorized into 2 groups: metallic (or plasmonic) NPs, and the others, including carbon nanostructures, quantum dots, rare earth (RE) containing NPs or polymer (organic) NPs. Based on different electronic structures involved, the absorbance energy parts from the incident light are transferred into heat (phonon) and/or luminescence. Taking under attention that, most photothermal studies have been dealt with metallic NPs, let us briefly describe the basic approach to understand the underlying mechanism of this case. As pointed out in Jauffred et al. [10], the dissipated energy Q can be written as:

$$Q = \iiint q.dV \tag{8}$$

where $q = \frac{1}{2}\mathrm{Re}(\mathbf{J}.\mathbf{E}^*)$ is the electric loss density within the nanostructure, integrated over the NP volume, $\mathbf{J} = \sigma\mathbf{E}$ is the current density as a function of the conductivity σ. In order to find the electric field **E** inside the NP, one has to solve the Maxwell equation:

$$\nabla \times \mu^{-1}(\nabla \times E) - k_0^2\left(\varepsilon^2 - i\frac{\sigma}{\omega\varepsilon_0}\right)E = 0 \tag{9}$$

Using adaptive refinements of the mesh sizes (finite element method - FEM), local electric field can be accurately solved not only for spherical NPs of various diameters but also for much more complex nanostructures. Having obtained the local E, the absorption cross section can be obtained by dividing the dissipated (absorbed) energy in the nanostructure, Q, by the intensity of the irradiating light I_o as follows:

$$C_{abs} = \frac{Q}{I_0} = \frac{1}{c\varepsilon_0|\mathbf{E}_{inc}|^2}\iiint Re(\mathrm{J}.\mathrm{E}^*)\mathrm{dV} \tag{10}$$

Using FEM to solve equation (10), one can not only reproduce the results obtained by Mie (see, e.g. [10]) using analytical approach and assuming the small size metallic NP (< 20 nm); but also apply for NPs of arbitrary size and shape.

The heating efficiency ϕ (defined as the ratio of extinction energy that transformed into heat) can be expressed as [11]:

$$\Phi = C_{abs}/C_{ext} \tag{11}$$

where C_{abs} and C_{ext} are, respectively, the absorption and extinction cross section.

The use of electromagnetic heating for processing of carbon nanostructures composite. Researches on using electromagnetic heating for curing, welding or repairing composite have attracted attention since several decades, and are still of much interesting. Attempts paid to

understand the heating mechanism, however, is not a simple task because composite is a non-homogeneous electrically conductive specimen. Moreover, the size of the conducting materials component like carbon fiber is thinner than the penetration depth to get large loop enough for generation of eddy current heating. In [21], the authors considered the case of possible two heating mechanisms, i.e. Joule heating within the carbon fiber component and dielectric loss heating in the polymer region for a thermoplastic specimen irradiated by an alternative magnetic field. The ratio of the dielectric power loss in the polymer matrix at j-th junction, W_j, to the Joule loss in the i-th fiber is estimated to be equal to [21]:

$$\frac{W_j}{P_j} = 3.35 \times 10^{13} h \tag{12}$$

where h is the thickness of polymer junction. From (12) it was deduced that the dielectric dissipation process dominates to avoid the dielectric breakdown.

Recent researches in nanotechnology have created various carbon nanomaterials including: carbon nanotubes (CNTs), graphene, graphite etc. Carbon nanostructures exhibit several new properties that can be beneficiated for addition to polymer to gain desired composite materials. For example, the interaction of CNTs with microwave can generate localized heating, which can be explored for applications in materials processing [22], including bonding, welding, curing thermosets, heating CNT/silicon. Very recently, researchers have found that RF electric fields of f = 1 - 200 MHz can be used to heat various carbonaceous materials including CNTs [23], graphene [24], carbon black [25], as well as carbon fibers [26]. In comparison with microwave, the RF–induced heating exhibits several advantages, such as deeper and better heating in thicker materials, better selectivity, shorter time and lower energy consumption. To stimulate such materials with an RF field, suitable electric applicators are required. Various contact or non-contact applicators used as electrodes have been developed to create electric linear field or fringing field in a variety of setups [4]. The mechanism of heating carbon nanostructures composite by RF electric field can be examined by treating the system as capacitor filled by a dielectric material. Heating response of the material depends on both field quantities (amplitude and frequency) and material properties. The quantity to determine the ability of material to be heated is it's dielectric loss tangent ($\tan ó = \frac{\varepsilon''(\omega)}{\varepsilon'(\omega)}$). For optimizing the heating efficiency, the material should exhibit a moderate value of ε' and high value of ε'' at the used field frequency ($f = \omega/2\pi$). The frequency dependence of the ε' and ε'' is relevant to the polarization processes involved in the material. In general, total polarization is composed of four sources: electronic polarization, ionic polarization, orientation polarization, space charge polarization. While electronic polarization appears in very high frequency range, the others do in microwave and RF ranges. For a single polar material the frequency dependences ε''(ω) and ε'(ω) obey Debye formalism, similarly to (6). In thermoplastics, e.g., orientation polarization relates to the conformation motion of polymer chains, and ionic polarization is due to the existence of ion salts as the impurity remained.

During the past 5 years, Green's group at Texas A&M University has carried out extensive studies of the RF heating of carbon nanostructures composites and concluded that it is possible to tune the conducting properties of this material to gain optimum RF heating efficiency [4]. Namely, the dielectric and conductivity properties can be tailored by addition of small amount of conductive carbon nanoparticles into (non-conductive) polymer matrix. The optimum heating efficiency occurs in the doping concentration of the transition region (percolation region) from dielectric range to conducting range, where the conductive filler network percolates [4]. In the dielectric region of low nanofiller concentration the heating is described by loss tangent tan ó,

whereas when the composite conductivity is high enough, the power loss density is proportional to the conductivity σ (originating from charge motion polarization),

$$Q = \frac{1}{2}\,\sigma|\boldsymbol{E}|^2 \tag{13}$$

The lowering of heating efficiency with further increasing conductivity in the conducting region can be explained by the decrease of penetration depth, d, (thickness of eddy current layer) which is inversely proportional to the conductivity,

$$d = \frac{1}{\sqrt{f.\sigma}} \tag{14}$$

By this assumption, the Green's group showed a good agreement between experimental curve and theoretical behavior of the dependence of heating rate on the conductive nanofiller concentration in the CNTs loaded nanocomposite [4].

The heating mechanisms, above discussed, for radio frequency AMF on MNPs (abbreviated as AMF@MNPs), light frequency AEF on PNPs (AEF@PNPs) and radiofrequency AEF on carbonaceous nanocomposite (AEF@C-nanocomp) were schematically presented in the last column of Fig. 1.

Table 1. Electromagnetic heating for different nanomaterials.

Nanomaterial	**Frequency range**	**Heating mechanism**	Ref.
Magnetic irradiating field			
Magnetic nanoparticles	RF	Hysteresis, Neel relaxation, Brown relaxation	[5, 16 - 18]
Electric irradiating field			
Metallic nanostructures	Light	Plasmon	[6, 7, 10, 11]
Carbon nanostructures & Carbonaceous nanocomposite	Light Microwave, RF	De-exitation process Dielectric polarization loss & Eddy current	[3, 4, 11]
Quantum dots	Light	-	[10, 11]
Organic NPs	Light	-	[11]
RE doped nanocrystals	Light	Upconversion dissipation	[10, 11]

2.2. Experimental characteristics

Due to the nanometer size as well as other specific characters of heat generators, the electromagnetic heating of magnetic nanoparticles and photothermal nanostructures demonstrate several advantages as compared with other heating technologies [4]. First of all, this is mainly a targeted technology, because the nanomaterials as a heat mediator can be localized very closely to the object heated. Secondly, the heating on and off can be controlled rapidly and remotely. Thirdly, the EM heating technique is efficient and economical due to the two previous advantages, i.e. the locality and rapidity.

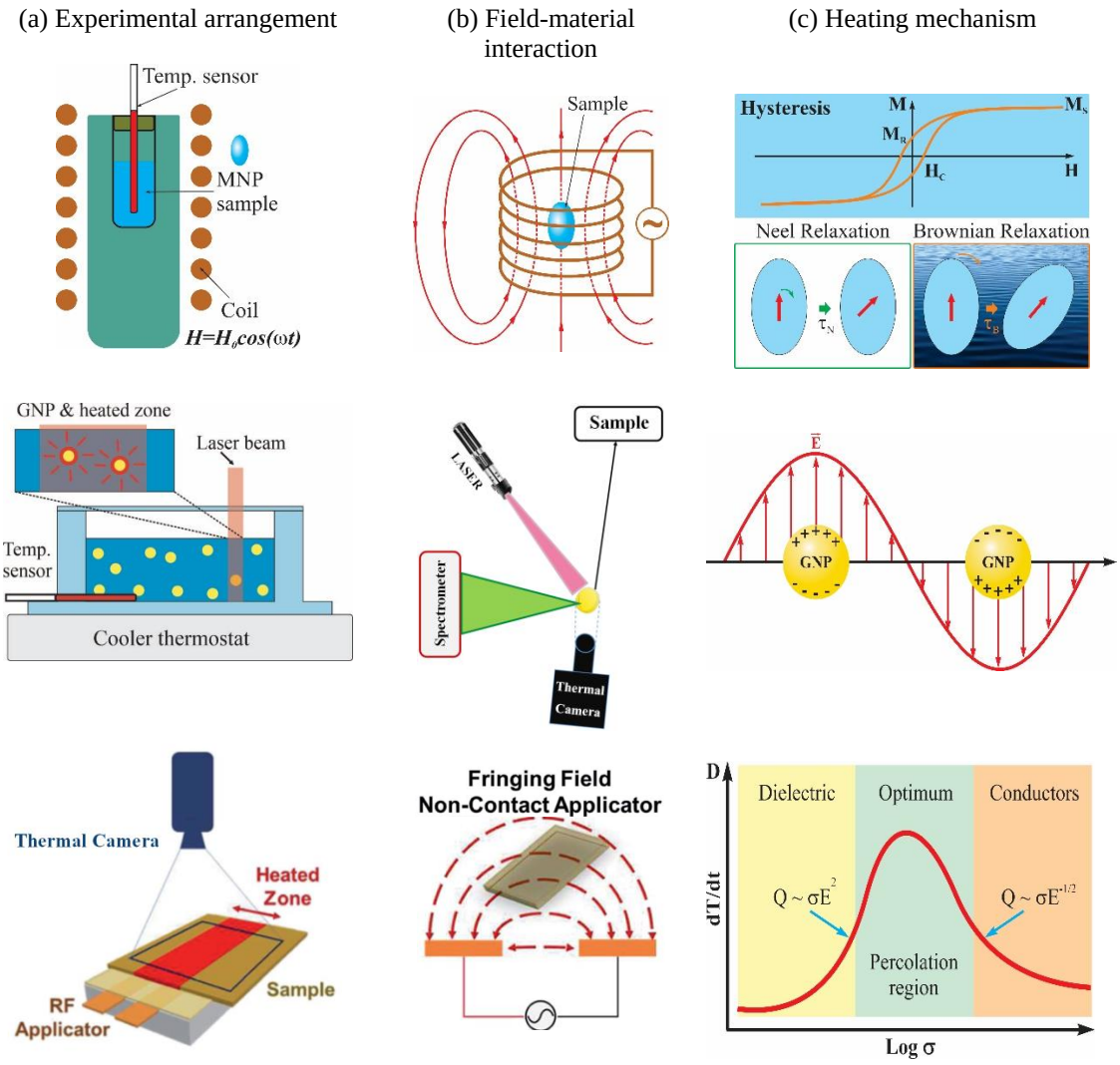

Figure 1. Schemes of experimental arrangement (a), field-material interaction (b), and heating mechanism (c) for 3 typical EM heating on nanomaterials: (upper row) AMF@MNPs, (middle row) AEF@PNPs, (bottom row) AEF@C-nanocomp. Adapted with modification from [4, 6].

There are also a few challenges that need to overcome, as follows: The heating equipment needs to provide field of enough good homogeneity in the sample/specimen volume. This requirement guarantees the sample not to be partly overheated which is dangerous in the case, e.g. of *in vivo* hyperthermia therapy. Another challenge is to ensure the efficient transmittance from the energy source to the energy receptor-convertor, i.e. the nanostructures. Namely, for the case of photothermal therapy, water containing tissues block the light wave, remaining two biological windows in the wavelength range of $\lambda = 700\,nm \div 980\,nm$ and $\lambda = 1000\,nm \div 1400\,nm$ [11], so that the photothermal nanoparticles (Au, e.g.) should exhibit high absorbance (plasmonic peak) in any of these window range. In practice, applications can be arranged by two approaches: guiding the EM wave directly to the heating component (using optical fiber, e.g.) or irradiating it remotely. The first approach is frequently used for single heating element, whereas the second one is for the volumetric heating case.

Instrumentation for research and applications. In general, an RF electromagnetic generator is designed by using an RLC resonance circuit, where R, L and C are resistance, inductance, and capacitance, respectively. The extraction of magnetic or electric field can be realized by using, respectively, an inductor or capacitor as output element or field applicator. In practice, the tuning of the field frequency is realized by variation of the capacity of conductor set or of the inductivity of the induction coils. Nowadays, while the RF generators for standard induction heating are commercialized, most of the experiments on heating nanomaterials by EM source are done on homemade equipment [4, 8]. For the purpose of studying magnetic heating in MNPs (AHF@MNPs), for example, while our group used the commercial RDO low power RF generator with 6-turns coil providing field of f = 130 - 400 kHz, H_0 = 40 - 100 Oe (3.18 - 7.96 kA/m) [27]; Fortin et al. [28] set a homemade system using a capacitor (10 pF - 4 nF) and inductance copper coil (25 μH, diameter of 16 mm) to gain the magnetic field of f = 300 kHz – 1100 kHz, and amplitude up to H_0 = 27 kA/m. Up to date, magnetic heating experiments performed by several groups reported the using AHFs of frequency and amplitude ranging, respectively, from about 100 kHz-1100 kHz, and 7.96 - 63.68 kA/m [29]. In each magnetic heating experiment, temperature increase must be recorded with the time since the switching on the field, and temperature increase rate (dT/dt) is analyzed for calculating the so-called specific absorption rate, SAR (the same quantity as specific loss power SLP), as follows,

$$SAR = (\frac{C}{m}).dT/dt \quad (15)$$

where C is the heat capacity of the fluid, and m is relative mass of the nanoparticles over the liquid mass. In order to compare the SAR data gained by different laboratories, it is useful to use so-called intrinsic loss power, ILP, as the parameter to characterize the heating capacity of magnetic nanoparticles under consideration,

$$ILP = SAR/f.H_0^2 \quad (16)$$

As for the clinical magnetic hyperthermia application, there is very little equipment developed until today, like the MFH (R) 300F set up constructed by Magforce Technology company (working at 100 kHz) [30], or MACH developed by Kallumadi at University College London described in (see e.g. [8]).

In photothermal experiment, the light source (AEF) commonly used to excite the heating in photothermal nanostructures (metallic NPs, CNTs, etc.) is frequently a diode laser or Nd:YAG laser [6, 10] of wave frequency in the near infrared range. The former is of a continuous modality while the second laser is of high power pulse modality (femtosecond pulse). Both these laser sources have some advantages in hyperthermia therapy, whereas for thermomagnetic memory application (see section 4.3) the pulse laser shows convenience in high speed signal processing.

Regarding the temperature measurements, various thermometers such as thermocouple, fluoro-optic or semiconductor diode, and thermal infrared camera have been used, with caution to choose proper device to avoid secondary effect like induction heating on the metallic part or optical induced dissipation in semiconducting component. There has been no report on any equipment developed or clinical photothermal treatment.

For studying nanocarbon composite heating, Green's group from Texas A&M University has recently developed three applicator sets to be used as capacitance electrodes, i.e. parallel plate non-contact applicator, fringing field non-contact applicator, and direct contact applicator [4, 31]. The matching of the RF source (AEF) impedance with that of the loading material, Z_s^* =' $Z_{L,}$ is a unique challenge because of the very sensitive change of conductivity in the

composite composition to the nanofiller concentration. These authors also used the nanocomposite composition variation along with the equipment network of variable inductor and capacitors for tailoring the impedance matching in order to get high heating efficiency for the 1-200 MHz frequency range. In all three applicator cases, the samples heat rapidly (heating rate over (100 ^{o}C/s) in response to the applied electric field of a few to hundred watts [4, 31]. It is worth stressing that the non-contact applicator configuration can be used for developing a continuous heating conveniently useful in industrialization [26].

The experimental arrangements, field-material interaction and the dissipation mechanisms for the above three heating cases are schematically presented, correspondingly, in the first (a), second (b) and third (c) columns of Fig. 1. It is interesting to notify that for the case of AEF@PNPs (middle row), with using an experimental set up like in Fig. 1, the generated heat can be measured accurately in adiabatic condition, and the temperature distribution can be recorded by using a Raman/fluorescence microscope [6].

The field frequency ranges to activate particular heating process in different nanomaterials are summarized in Table 1.

3. NANOMATERIALS FOR ELECTROMAGNETIC HEATING

The huge potential applications especially in biomedical field have caused an explosion of researches during the past two decades in developing new methods for synthesizing nanostructures of various design and different compositions. In order to have a general view on the materials parameters affecting the NPs-based heating efficiency, we endeavor to summarize the magnetic and photothermal nanostructures, respectively, in Tables 2a and 2b.

3.1. Magnetic nanoparticles

As shown in Table 2a, almost all of the magnetic nanostructures studied in electromagnetic heating are of oxide compounds with 3 dimensions nano limited in size, i.e. nanoparticle. Oxide magnetic nanoparticles can be synthesized by different methods including: co-precipitation, hydrolysis, thermal decomposition, sol-gel or liquid plasma ablation, etc. [9, 12]. The first two techniques, co-precipitation and hydrolysis are simple and facile techniques, which produce nanoparticles of spherical shape of wide range in size. In order to get nanoparticles of better crystallinity and of controlled shape (cube, flower) thermal decomposition method is a better option. The drawback of this technique is that it needs a step more to eliminate or exchange the organic solute remaining as a coating layer on the formed particle surface.

A lot of attempts have been made to synthesize spherical NPs with varying the diameter parameter d to verify the SAR(d) dependence predicted by LRT theory (see e.g. [16]). It is, however, not easy to experimentally cover the maximum SAR region by tuning only the particle diameter [32 - 34], as it is extremely hard to keep the nanoparticle anisotropy parameter, K, constant (or monotonic variation) for various size or by different experimental batches. In order to tune the K parameter for exploring other magnetic effects including hysteresis dissipation and/or exchange bias, more complex particles such as cubic, flower, core-shell magnetic systems have been synthesized and their heating SAR studied [35 - 43]. To the best of our knowledge, the best heating efficiency reported up-to-now was for the case of $Zn_{0.4}Fe_{2.6}O_4$-$CoFe_2O_4$ hybrid soft core – hard shell with cubic morphology system [36b], so that the recorded value SAR = 10600 W/g (ILP = 14.9 nHm^{2}kg^{-1}) (Table 2a). The exchange bias induced in such hybrid

nanoparticle along with the high coercivity (H_c) were assumed to give a big hysteresis contribution, whereas the cubic shape to produce high magnetization, which all result in very high heating efficiency. Regarding the shape dependence, it is interesting also to draw attention on the observation of systematic increase of the SAR parameter with increasing aspect ratio of magnetic Fe_3O_4 nanoparticles that has been recently reported by Mohapatra *et al.* in [39] (see also Fig. 2a).

Table 2a. Shape and composition dependence of heating efficiency of magnetic nanoparticles.

Magnetic nanoparticles	Shape	Size (nm)	Magnetic field, f(kHz) /H(kA/m)	SAR (W/g)/ILS (nHm^2kg^{-1})	Ref.
Fe_3O_4,	Spherical	10	265/39	475/2.1	[39]
Fe_3O_4	Cube	19	520/29	2452/8.6	[40]
		20, 40	765/(12-24)	(150-500)/(1.4-1.1)	[37]
	Nanowire	10 diameter 25 length	265/39	846/2.1	[39]
Fe_3O_4	Multi-core	29 (10 SNP) 50 (14 SNP)	520/29 400/25	1500/3.4 400/2.8	[43] [42]
γ-Fe_2O_3	Nanoflower	25 (11 SNP)	700/21.6	1992/6.1	[41]
FePt-Fe_3O_4	Core-Shell Cube	14.7	630/18.9	1210 /5.4	[38]
Fe_3O_4-$MnFe_3O_4$	Core-Shell Sphere	15	500/36.8	2785/4.0	[36a]
$CoFe_2O$@$MnFe_3O_4$	Core-Shell Sphere	15	500/36.8	2280/3.3	[36a]
$Zn_{0.4}Co_{0.6}Fe_2O_4$-$Zn_{0.4}Mn_{0.6}Fe_2O_4$	Core-Shell Sphere	13	500/36..8	3886/5.6	[36a]
$Zn_{0.4}Fe_{2.6}O_4$-$CoFe_2O_4$	Core-Shell Cube	70	500/37.7	10600/14.9	[36b]

SNP – single NP.

Although it is theoretically well known that loss power is proportional to the particle magnetization M [20], and metallic magnetic materials such as Fe or FeCo exhibit very high M values, magnetic heating of those metallic nanoparticles has been very little studied because their M is strongly decreased in magnetic nanofluids. As for the field parameter dependence, the linear increase of energy loss power with frequency has been indicated both by theoretical and experimental observation. The SAR (or SLP) vs squared field amplitude (H_0) behavior indicated by the LRT theory has been confirmed in many experimental reports carried out for superparamagnetic nanoparticles in the small field region.

It should be notified that while MNPs of high SAR values are of good choice for any *ex-vivo/ in vitro* applications, the nanoparticles characterized by high coercivity H_c and their SAR gained by measurements in high f and H_0 should be treated with caution in the case of *in-vivo*

applications. The reasons are that particles of high H_c still remain magnetized after switching off the external field, and there is a so-called biological limit stating that the product $f.H_0$ of used field should be smaller than 4.85×10^8 A/(m.s) [44]. Nevertheless this criteria is under debate to increase of one more order or so (5×10^9 A/(m.s) [45], (9.59×10^9 A/(m.s) [46]).

3.2. Photothermal nanomaterials

Specific optical properties of nanoparticles, including metallic and semiconductor were known and applied for several centuries and recently intensively studied along with the explosion of nanotechnology. However, for a long time the light absorption and then its conversion to heat have been considered as a side effect in applications. Intensive research on photothermal heating has been explored since the beginning of this millennium, especially after scientists demonstrated that the heat generated on metallic nanoparticles is not only of a temperature increase sufficient for biomedical treatment (around 10 degrees), but even can cause massive phase transformations in a surrounding material such as ice or polymer [6].

Up-to-now, extensive researches have shown that significant photothermal effect is observed in several nanomaterials (Table 2b), which can be categorized basically into two groups, i.e. metallic or plasmonic nanoparticles (such as Au, Ag, Pt, TiN, etc.) [47, 48], and non-plasmonic namaterials composed of a number of classes: carbon-based nanoparticles (CNT, graphene, black carbon) [49], semiconductor nanocrystals (quantum dots, chalcogenides) [47], Rare Earth doped nanocrystals [47], and even organic nanoparticles [50]. The synthesis, spectroscopy and potential applications of these photothermal nanomaterial classes are overall summarized in review articles [10, 11].

3.2.1. Plasmonic nanoparticles

The most interesting and widely studied photothermal effect group is undoubtedly the metallic nanoparticles. Different from bulk sample, the light-induced heating of metallic nanostructures becomes strongly dependent on both the irradiating wavelength and the size and shape of the nanoparticles.

Typical example is the systematic shift of the absorption peak (localized surface plasmon resonance - LSPR) observed, e.g., to situate at λ_{LSPR} = 521 nm for Au spherical nanoparticle of diameter d = 22 nm, towards λ_{LSPR} = 575 nm for nanoparticles of d = 99 nm [48]. Although the increase of plasmon peak wavelength via increasing sphere diameter of gold nanoparticles (GNP) is limited at about 600 nm, it is fortunate to obtain absorption peak appearing in NIR region by another approach, namely to fabricate metallic nanoparticles with more complex geometries such as: nanorods, nanocages, nanostar or core (silica)-shell (gold) nanoparticles [10, 11]. For gold nanorods (GNR), e.g., the absorbance spectrum is characterized by two peaks, namely a strong peak appearing in the NIR region, which originates from the oscillation of electron along the long nanorod axis, and a weak peak situated in the visible region, which is relevant to the oscillation of electrons along the short dimension [48]. The longitudinal peak is strongly red-shifted with increasing nanorod aspect (length/radius ratio). This tunability of plasmon peak of GNRs into the NIR region, i.e. the so-called second biological window, is particularly suitable for photothermal therapy application, which will be presented in more detail in 4.1.2 subsection. As for light-to-heat conversion, the heating efficiency coefficient for various shapes of Au NPs is linearly increasing with the laser intensity so that the highest efficiency (ϕ of around 100 %) was gained for core-shell nanostructure (Fig. 2b [51]).

Table 2b. Shape & composition dependence of heating efficiency of photothermal nanomaterials (Adapted from [11] with modification).

Photothermal nanomaterials	Shape	Dimension (nm)	Light wavelength λ (nm)	Heating efficiency: a_{abs} (cm^2) /ϕ	Ref.
Plasmonic nanoparticles					
Metallic GNPs	Spherical	22 99	808	Ext 1×10^9 (for GNP d = 20 nm)	[48a] 48b]
	Rods	8 width 29 length	808	4.3×10^{-11}/0.96	[51]
	Core@shell	120 Si- core 10 Au shell	808	10×10^{-11}/0.67	[51]
	Star	38 core 9x46 lobes	808	4.4×10^{-11}/1.0	[51]
	Cage		808	3.1×10^{-10}/0.62	[51]
Non-plasmonic nanomaterials					
Carbon Nanostr.	Tubes Graphene	0.6 radius 150 length	808	1.5×10^{-14}/0.5	[52a] [52b]
Quantum Dots	CdS Sp CuSe Sp	2 radius 8 radius	- 970	1.8×10^{-16}/0.14 6.5×10^{-14}/0.22	[53]
RE Doped Nanocrystals	$Nd^{+3}YF_4$	20 radius	808	$\approx 10^{-14}$ /-	[54, 55]
Organic dye	PEDOT:PSS	80-90 radius	808	Temperature increase 25 °C	[50]

3.2.2. Carbon nanostructures

Similar to the case of metallic NPs, light-induced heating of carbon-based nanostructures is a topic of extensive studies due to its various potential applications. Among a number of carbon-based nanoparticles, nanodiamonds exhibit no significant light-to-heat conversion efficiency whereas CNTs and graphene have shown remarkably high heating effect. CNTs are cylinders of graphene rolled in a tube of tens nanometers in diameter and microns in length. Different physical, mechanical, electrical, and optical properties of CNTs can be tuned via varying geometrical parameters such as 'chiral' angle and curvature of the rolling. For instance, depending on the so-called chiral vector *(n,m)* index, the CNTs can have conductivity of metallic or semiconducting character. In practice, the existing technologies frequently produce a mixture of CNTs with different chirality indices, which consequently makes the product not easily to predetermine of metallic or semiconductor properties. Low cost and mass production technologies produce nanostructure of multi-walled carbon nanotubes (denoted as MWCNTs). Besides CNTs, graphene layers have been shown to exhibit outstanding absorption properties also in the NIR region [52]. Light-to-heat conversion in CNTs is due to de-excitation processes

between so-called Van Hove states [11]. Heat is produced by the non-radiative relaxation of surface current. Extinction spectra of graphene-related nanostructures show that they present advantage of tunable photothermal heating in a wide wavelength visible-infrared region (including the second biological window).

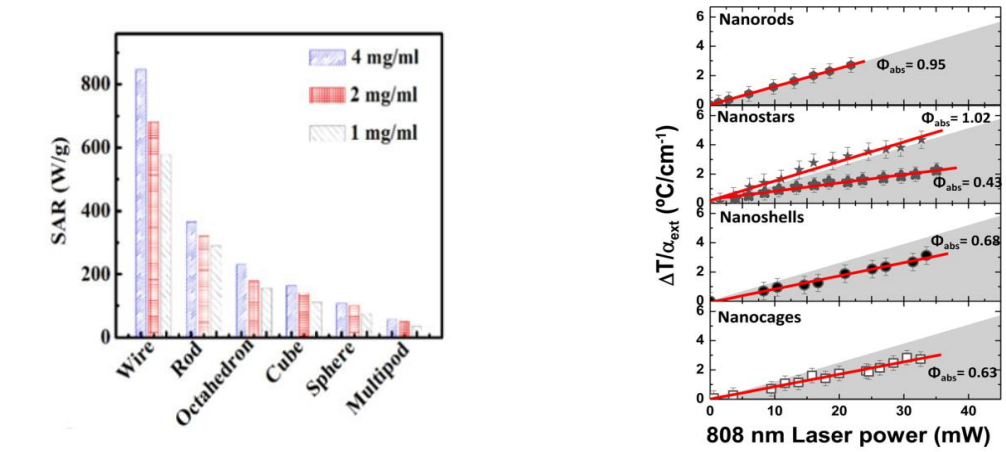

Figure 2. Specific absorption rate SAR of Fe_3O_4 NPs (a) and Absorption efficiency ϕ of gold NPs (b) for various particles geometries, Reproduced from Refs. [39, 51].

As shown in Tab. 2b, the light-induced heating efficiencies of different nanomaterials can be arranged in the following sequence: (Au) metallic NPs>Carbon-based NPs> QDs & RE NPs> Organic NPs. It is worth notifying that, despite the absorption efficiency of CNTs lower than that of GNPs, CNTs have the advantage of much broader spectral tunability for extinction and absorbance.

The heating of nanomaterials presented in sections 3.1 and 3.2 is induced solely by respectively magnetic AMF (RF range) and AEF (light range frequency). In order to beneficiate the two effects on the same nanomaterials, several hybrid and/or composite nanostructures composed of magnetic and photothermal components have been developed recently [56 - 59]. The simultaneously irradiation of magnetic and light on these materials have shown, indeed, that the heating efficiency has been increased much more than by using solely one of the sources. Interestingly, Espinosa group found and other groups confirmed, that the SAR quantity of Fe_3O_4 NPs much increased under simultaneously irradiation of a laser and an AC magnetic field in comparison with using a single stimulating field [56].

3.3. Composite nanomaterials

The above mentioned materials are the nanostructures of electromagnetic heating oriented mainly for the therapy application purpose. For material processing, the requirements like toxicity, purity, stability etc. are no longer strictly demanded, so that a few more EM heating nanomaterials (such as: black carbon, non-noble metallic NPs, etc.) can also be involved.

Nanocomposites are composed of polymer matrix with various additive materials of nanosized structure. As for magnetic nanocomposites, different magnetic nanoparticles such as Fe_3O_4 [60], $BaFe_{12}O_{19}$ [61] and metallic Fe [62] have recently used as magnetic filler to create functional materials. In these nanocomposites AC RF magnetic field (AMFs) can be applied

very efficiently to stimulate Neel relaxation- and hysteresis-based heating for the polymer curing [5]. On the other side, carbon-based nanomaterials, especially CNTs, have been shown to serve as really good additive/filler for the nanocomposite, for which rapid heating can be achieved by using electromagnetic field of frequency below 300 GHz [4]. The heat generation in a CNTs containing media was first found in microwave range, which is interesting for applications not only in biomedicine but also in materials processing [63, 64]. During the past decade, researchers (especially the Green group from Texas A&M University) discovered that RF electric fields in the range of 1-200 MHz can be used to process composites containing carbon nanomaterials including CNTs, graphene, carbon black and carbon fibers [4, 64, 65]. In [65], by performing experiments and simulation studies, for wide range of nanomaterials loaded composites; the authors found that the RF heating rate is non-monotonically related to the conductivity of the materials. Maximums heating rate appears at an optimum DC surface conductivity, which is the same for thin films made using the corresponding nanocarbon materials (CNT, graphene, carbon black), and is closely correlated with the percolation threshold in a given structure. This finding provides a key to optimization of RF heating for enhancing efficiency in RF–based materials processing technique.

The ability of heating generation in RF region can provide key advantages over that in the microwave range, which open a wide range of applications in materials processing, that will be discussed in the following section 4.2.

4. APPLICATIONS

4.1. Biomedical applications

The use of heat for the purpose of therapy is well known in ancient history, and that of EM-induced heat source was initiated yet in the 19^{th} century [2]. In the present nanotechnology era, the thermal therapy has been renewed because the heat sources (the nanoparticles to convert EM energy to heat) now become the size matching to those of biological objects, and moreover they can be localized closely to the cancer cells/tissues. Thermal treatments (TT) are based on driving parts of body above its normal temperature to cause cells killing or modification. There are three TT categories including: (i) diathermic treatment (temperature elevation up to 41 ^{o}C), hyperthermia treatment (41 - 48 ^{o}C), and irreversible thermal treatment (above 48 ^{o}C for short time). With possibilities of localizing and fast controlling the heat sources, nanoparticles-mediated EM TT are invasive and safe therapy methodology, which can avoid side effects. In literature, special focus has been paid to cancer therapy using magnetic hyperthermia treatment (MHT) and photothermal treatment (PTT).

4.1.1. Cancer therapy by MHT

The concept of using MHT for cancer therapy was initiated in 1957 by Gilchrist et al. [66] via performing *ex-vivo* introduction of γ-Fe_2O_3 MNPs into lymph nodes and then irradiating the animal with a magnetic AC field of f = 1.2 MHz, H_o = 16 - 19.2 kA/m to gain temperature increase of 14 ^{o}C for treatment of cancer metastasis. Since mid-1990 quite a huge number of researches have attempted to fabricate MNPs with improved heating efficiency (higher SAR) as well as demonstrated their potential for MHT of cancer tumor [67 - 73]. A good review on state-of-the art *in-vivo* experimentation of MHT is in [7].

Although first trial on clinical application of MHT was conducted about 15 years ago [73] little progress has gained since then. Firstly, it requires that the MNPs should be of superparamagnetic character, and secondary, the product frequency by amplitude of applying magnetic field (AMF) should not exceed the biological limit, i.e. $fxH_o = 4.85 \times 10^8 A/(m.s)$, major researches reporting MNPs of high SAR values (Table 2a) unfortunately involve nanoparticles of magnetic character and field applied that are out of the above requirements. As for the magnetic material, iron oxide of magnetite (Fe_3O_4) or maghemite (γ-Fe_2O_3) in form of spherical nanoparticles with small diameter (< 20 nm) have been safely chosen for *in vivo* applications.

Other challenges are that: (i) aggregation of the nanoparticles in real biological media might much influence the heating efficiency, and (ii) it is hard to measure in real-time the tumor temperature to estimate the temperature dose sufficient for the thermal hyperthermia treatment ($T(tumor) = 41 - 48\ ^oC$). A promising approach is to use magneto-fluorescent hybrid nanoparticle for simultaneously magnetic heating and temperature feedback monitoring, but it might demand sophisticated devices in instrumentation [75]. In [75], Luengo *et al.* proposed a practical approach, namely to adjust the tumor temperature via finely adjusting the magnetic field amplitude in real time. This proposal seems really promising for future implementation of the MHT for cancer therapy.

4.1.2. Cancer therapy by PTT

The application of PTT to cancer therapy was first proposed in 2003 by two research groups in the USA. Pitsillides et al. [76] used 20-nm spherical GNPs and 20 ns pulse Nd:YAG laser of 532 nm wavelength to *in vitro* study the killing of blood lymphocytes cells, whereas Hirsch et al. [77] used nanoshell of silica-Au injected into tumor volume, and irradiated with 4 W 820 nm laser light to *in vivo* observe irreversible thermal destruction of solid breast tumor. Since then, extensive research has been conducted to improve the heating efficiency (HE) and tumor accumulation (TA) of the PTT agents, as well as those towards clinical trials [78 - 82]. Among them, developments of nanosized photothermal agents of higher HE, higher TA and capable to integrate multiple imaging modes and therapeutic functions into one platform have drawn special attention. As summarized in the review paper [80], the multifunctional nanoplastforms include almost all the photothermal nanostructures discovered (i.e. GNP, GNSt, GNC, GNRs, hollow gold NPs, single wall carbon nanotubes, nanographene oxide, upconversion nanoparticles, and tungsten sulfide QDs) carrying functional agents such as: doxorubicin and paclitaxel, urease B, indocyanine green, thermal responsive liposome etc. Recent studies have demonstrated the benefits of combining PTT with other therapeutic modalities, including photodynamic treatment (PDT), chemotherapy (CT), radiotherapy and immunotherapy [80]. Multimodal therapies provide opportunities to exploit the advantages and avoid the drawbacks of each single modality, leading to additive and synergistic therapeutic effects [80, 82]. For instance, the simultaneous use of PTT with PDT can help to decrease the laser intensity and shorten its irradiation time compared to using PTT or PDT alone. Whereas, PTT can induce physiological changes (permeability of blood vessel, cell membrane, etc.) that could boost the CT effects by increasing the anticancer drug accumulation in tumor tissue or metastatic tissue.

It should be mentioned that, NPs such as CNTs upon the reaction with electric field of lower frequency range could result in a heating dose sufficient to use for destroying cancer cells as demonstrated in the work by [83], nevertheless the used RF power of 600 W at 13.56 MHz seems quite too large.

Although the reports showed some promising results of using PTT for cancer, clinical implementations are still lacking and face obstacles that need to overcome. Several limitations remain to be addressed, especially the delivery (targeting and accumulating) of the PNPs at the tumor site [13, 81]. In a very recent review paper [81], the authors summarized a list of different strategies for efficient delivery of PNPs including: intratumor injection, passive (functionalization of PNP with targeting moiety) or active targeting (driving magnetic hybrid PNP by external magnetic field, e.g.), biomimetic targeting, and programmed targeting. Intratumor administration has been used in almost all the animal PTT experiments of solid tumors because the devouring effect of the RES system can lead to small amount of PT agents remaining in the tumor volume shortly after intravenous injection. The later administration strategy has been applied in a few papers reporting promising success of PTT application for some metastatic cancers.

As reviewed by Han *et al.* [80], only four recorded (during the past 5 years from 2016 to 2020) pre-clinical studies demonstrating the use of 150 nm silica-gold nanoshell as PTT agent (developed by Nanospectra Biosciences) to intravenously inject into the bloodstream and to irradiate with 808 nm laser, which leads to cell deaths and tumor regression of metastatic lung tumor, head & neck tumor or prostate cancer [80].

4.1.3. Other biomedical applications of EMH

Due to a variety of the thermal response of biological materials, magnetic heating (MH) and photothermal heating (PTH) can be used in several other biomedical applications including: remote control of gene regulation, sterilization/disinfection [13], and of membrane heating [10, 13], molecular or drug release [10, 84 - 89, 90 - 94], and rapid rewarming of vitrified biomaterials [95 - 100]. Let us briefly review some results achieved for the two last domains of applications.

Remotely controlled release of drugs inside living organisms is particularly attractive because it would allow the drug accumulation at exact site and time of necessary. For this purpose, much effort has paid into developing on multifunctional nanoplatforms based on both MH [84 - 89] and PTH [90 - 94] agents.

For instance, in [89] the authors loaded curcumin into co-polymer coated MNPs, i.e. Fe_3O_4-(PLA-PEG)/curcumin, demonstrating that this model drug can be released remotely by using a weak magnetic field (178 kHz, 5.0 kA/m)) with much higher efficiency than that done by passive releasing. After 20 min under applied field, the curcumin amount loaded in the Fe_3O_4-(PLA-PEG)/Curcumin has been almost fully released, whereas the released amount by passive heating approach reached only 80 % after 24 h.

In [91], short RNA strands were released from surface of gold nanostars and gold nanorods upon laser irradiation, where one strand RNA attached on the surface via a thiol bond. The release mechanism was supposed to be of thermal activated dehybridization of the RNA molecule. Another interesting plasmonic nanocarrier is a gold nanostar core shelled with a layer of mesoporous silica, where doxorubicin is loaded and the whole is coated by outmost layer of paraffin; so that upon irradiation of NIR laser the paraffin partly melts and releases the chemotherapeutic drug [94]. Lipid membranes including plasma membranes undergo phase transition from gel to fluid state by a moderate temperature increase. It has been demonstrated that the permeability of the membrane can be remotely increased by irradiating RF magnetic field or laser light, respectively, onto the Fe_3O_4 NPs [87] or Au NPs [92] that were trapped on the membrane surfaces.

Another biomaterials group that needs, in contrast, to increase the heating volume is the biospecimen (living tissue/organs) cryopreserved for long term by vitrified deep cooling to be rewarmed before using in transplantation medicine. Earlier attempts done to use traditional warming techniques such as using warm water bathing or using radio frequency heating [95], beneficiating the electric field interaction, failure to rewarm biospecimen of over 3 ml in volume. Very recently, a new innovative approach was introduced, firstly by Bischof group in 2014 [14] to apply radiofrequency magnetic heating for rewarming specimens containing magnetic nanoparticles [96 - 98], that up-to-date can successfully devitrificate such large biospecimens as a rat kidney [99, 100]. The key parameter to achieve is that the warming rate should be higher than a critical value (order of hundred ^{o}C/min) to avoid devitrification during thaw. Despite the fact that previous attempts of using high frequency (MHz, GHz) could gain heating rate up to hundred ^{o}C/min, the failure in increasing heating volume is due to spatial variations of the dielectric properties of tissue as well as inhomogeneity of electric field distribution in the specimen volume. Using AC magnetic field of lower frequency (< 1 MHz) can avoid these limitations to create heating uniformly on much larger biospecimen. Namely, the authors used spherical Fe_3O_4 NPs of 10 nm in diameter to mix with cryoprotectant VS55 solute to make vitrification solution (concentration of up to Fe 10 mg/ml) for cryopreservation cooling of biospecimens (porcine artery, heart leaflet tissue). Then an AMF of 360 kHz/20 kA/m was applied to get heating rates up to 300 ^{o}C/min, which is of 4-5 times higher than the critical warming rate for that cryoprotectant (55 ^{o}C). By this approach, the rewarming could be successfully conducted for biospecimens of volume up to 80 ml [97]. As indicated in [99, 100], by using similar approach these authors very recently demonstrated successful nanowarming of the whole frozen rat kidney, so that the maximum thermal stress of the organ was reduced by two orders in comparison with that caused by water bath thawing. The updated results reported by independent laboratories suggest that kidney nanowarming holds tremendous promise for transplantation.

4.2. Electric heating for nanocomposite processing

While magnetic heating has been very rarely applied for the polymer/composite processing [101] the heating by electric field, especially that in RF range, used for nanocomposite processing has recently been extensively studied. During a short period of only 5 years from 2017 - 2022, the Green's group from Texas A&M University has achieved much successes with the research and development of the RF heating technique for various nanofillers aiming at different materials engineering as reported in [4, 24, 31, 64, 65, 102 - 104]. Namely, in [64], the authors made MWCNT coating on polymer filaments to fabricate 3D-printed parts, and locally RF heating them, which results in strengthening of the interfaces with fracture strength increased by 275 % over baseline 3D parts. This locally induced heating is capable of increasing the interlayer bond strength without sacrificing the dimensional accuracy of the part, which is applicable for parts of complex shapes. In [31] Sweeney et al. used nanoadhesive of CNT (2 %)/polylactide thermoset to bond aluminum substrates upon irradiation of electric field of power 100 W, frequency around 100 MHz, and achieved rapid heating of nanoadhesive without heating substrate and not depending on the field applicators. A demonstration example was shown to use a high performance epoxy loaded with MWCNTs to fast and well joint the bed of a truck chassis. Gerringer *et al.* [24] made graphite structures from various industrially prevalent thermoplastics to show their rapid heating (of rate up to 124^{o}/s) using RF power of < 30 W, around 100 MHz, resulting in fast and selective welding of polymer-polymer interfaces. After 150 s of heating the welded samples possess an average strength of 12.86 MPa. Vashisth *et al.*

[104] used RF field of around 100 MHz & nanocomposite adhesive to bond substrates of different metallic materials. The RF cured multi-material bonding exhibited minimal distortion (aluminum-to-steel specimen), with fracture energy of 590 higher than oven-cured specimen. The finding is to be applicable in joining dissimilar materials like aluminum and reinforced plastics in automotive and construction industries.

As highlighted in the review paper by Vashisth *et al.* [4], carbon nanomaterials rapidly evolve heat in response to RF field (1 - 200 MHz), which is the safer range and more versatile compared with microwave. The found behavior that various nanomaterials, dispersed in different matrix (polymer, ceramics) of these composites rapidly heat upon irradiation of RF field is valuable for materials processing, where volumetric and/or targeted heating desired, including: curing composite, bonding multi-materials surfaces, additive manufacturing, along with medical ablation (Fig. 3, [4]). The heating using RF electric fields can circumvent a number of challenges faced by conventional techniques such as oven, furnace or IR lamp. Among the advantages, one can mention the following [4]:

(1) Faster heating time: Using RF field to plastic substrates, their temperature could reach the temperature required for bonding (80 ^{o}C) within 45 s, which is 6 times faster than that by IR heating. For carbon fiber/epoxy the curing time necessary can be achieved for 2 min by RF heating, which is about 10 times shorter than by conventional oven.

(2) Targeted heating: allows to heat specifically localized in assembles bypassing heating other components to avoid thermal stresses.

(3) Flexible tailored response: For polymer composites, for given set of frequency and input power, it is possible to achieve the desired heating rate via tuning the composite nanofiller concentration. For example, heating rate increases from 0.1 ^{o}/s to 30^{o}/s for increasing MXene concentration from 1 wt.% to 25 wt.%. Other option is to change field parameter, e.g. heating rate varied from 0 - 10^{o}/s when frequency varies 1 - 200 MHz at power of 2 W.

(4) Low infrastructure: The method allows out-of-oven rapid processing, thus mitigating the need for large ovens or autoclaves.

4.3. Other miscelllaneous applications

Apart from the applications in biomedicine and composite processing domains presented in the sections 4.1 and 4.2, the nanomaterials-mediated EM heating shows up yet to possess a number of other miscellaneous applications as discussed in several review and research papers [13, 10, 105 - 109]. An interesting example is a potential application of magnetic heating in environment [107 - 109], namely to use zinc-substituted ferrite NPs [108] as nanoheating agent to mix with absorbent materials (such as active carbon [107], SBA [109]) for desorbing the adsorbed toxic solvent (such as benzene, m-xylene) for regenerating the materials. This inside-to-outside heating approach was shown to exhibit several advantages, such as lower cost, faster desorption, higher efficiency etc., as compared to traditional use of water vapor for the purpose. For the case of photothermotics, several exotic applications such as: photothermal and hot-electron chemistry, solar light harvesting (including thermophotovoltaics, nanofuids for solar energy harvesting, water desalination) or thermal induced liquid flows were outlined [13].

As a strong heating is produced by irradiated PT agent, especially plasmonic NPs, steep local thermal gradient could be created, which can be exploited in optofluidics or optoelectronic devices. We want to draw attention to two applications related to beneficiation of temperature gradient at nanoscale and microscale as follows.

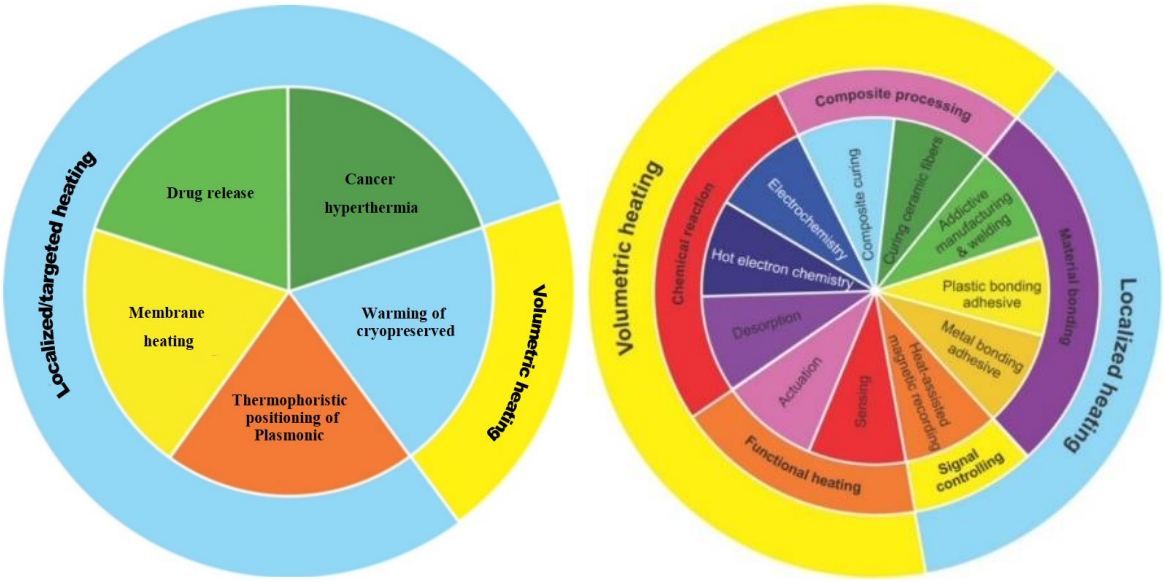

(a) (b)

Figure 3. Applications of nanoparticles-mediated EM heating in biomedicine (a) and in materials processing (b).

a) Optothermophoresis

In fluids, a temperature gradient ΔT causes a migration of solute which follows Ludwig-Soret law, $v = -D_T.\Delta T = S_T.D.\ \Delta T$, where: v is thermophorestic velocity, S_T is Soret coefficient, D_T is thermophorestic mobility, and D is solution diffusion coefficient. Plasmonic nanostructures can create such a steep ΔT to cause colloid convection of speed up to 1 μm/s [10]. Optical trapping effect of AuNPs upon irradiating showed up to be potential for various applications, e.g. to use thermophoresis force to fine-tune the particles position along the axial direction of the laser beam [10, 110]. A practical application example of this kind technique is to precise position NPs before injecting them into the cytoplasm [10]. When plasmonic NPs are positioned between vehicles or cells, these biological objects can be fused by the photothermal heating so that the vesicle cargoes or cell cytoplasms become mixed from each vesicle/cell to the other. Plasmonic optical trap and cell fusion, thus, pave the way for a number of novel future applications.

b) Optospincalorimetric

Seebeck effect is a well-known phenomenon saying that when two conductors of different Seebeck coefficients are connected with each other, an electronic voltage is created between their outputs which is proportional to the temperature difference between the ends of the couple. In 2008, Maeda group [111] discovered so called spin Seebeck effect stating that, in a metallic magnet, the spin up (↑) and spin down (↓) conduction electrons have different Seebeck coefficients, so that a spin voltage $\mu_\uparrow - \mu_\downarrow$ is created which is proportional to the temperature difference. In 2014, Choi *et al.* [112] demonstrated the observation of spin current generated by thermally driven ultrafast demagnetization in a metallic multilayer system with Pt as a plasmonic nanoheater and CoPt and CoFeB as ferromagnetic layers. Temperature gradient ΔT of up to 90 K was attained by using a laser density of 17.3 J/m^2, 785 nm in wavelength, nanosecond pulse. Very recently, Bello *et al.* [15, 113] used a laser of 2.75 mW, 850 nm, picosecond pulse to generate a temperature gradient of 30 - 40 K/nm in a system of Au layer (plasmonic mode)

coupled directly with a Near-Field-Transducer (photonic mode), observing the switching field effect which is applicable in heat-assisted magnetic recording (HAMR) technology.

The RF magnetic heating applied in desorption and light plasmonic heating used in thermophoresis and thermospintronics can be properly assigned into application categories along with the domains discussed in sections 4.1 and 4.2, as shown in Fig. 3a and 3b.

5. SUMMARY AND OUTLOOK REMARKS

In this review, we used a concise approach to present the strong absorption responses of various nanoparticles to the electric and magnetic fields, namely: MNPs in AMF of RF range, PNPs in light frequency range, and nanocarbon-based composites in AEF of RF range. Extensive studies on improving the heating efficiencies of AMF@ MNPs and light or AEF@PNPs have resulted in fabrication of agents with high specific low power values, and demonstrated the techniques efficient in treating cancer in mouse model systems. There are still challenges to overcome on the way to implement the magnetic and photothermal heating methodologies into clinical applications, e.g., it is necessary to establish a more efficient strategy for delivery of nanoparticles, and/or to perform a direct temperature measurement at the tumor site. The nanoparticles-based hyperthermia of cancer is undoubtedly so promising that continues to be a hot research topic in near future. Apart from cancer therapeutics, the nanoparticles-assisted electromagnetic heating also has numerous other exiting applications. The AMF and/or AEF heat-triggering of drug release provides another promising methodology for synergetic treatments by hyperthermia combined with another therapy such as chemical or radiological ones. The usage of RF AMF@MNPs for desorption of solvent adsorbed on adsorbent materials is an example of efficient application of volumetric heating in the field of surface chemistry. We have presented two cases of exotic applications relevant with the possibility of creating steep (nanoscale) temperature gradient by single plasmonic nanoheater, i.e. thermophoresis and thermospintronics, which is expected to grow considerably in the near future. Finally, most recently developed using of RF AEF@C-nanocomp has suggested huge promising to apply the EM heating technology for volumetric processing of nanocomposite and/or for localized processing of components in multimaterial manufacturing.

Along with the heated targeting, another striking advantage of EM heating, which is common for all the susceptor nanomaterials and both the AMF and AEF is the strong reduction of process time. A molecule release can be performed 50 times faster, or a bonding/curing polymer composite can be realized for 6-10 times shorter as compared with using traditional heating technology. The largest challenge of the technology is the real time control of the heated temperature in *in vivo* applications. To our guess, the domain of RF AEF@C-nanocomp heating might be implemented into industry earlier than that of therapeutic purpose.

Acknowledgement. The authors acknowledge the AOARD grant FA2386-17-1-4042 and the VJST journal for the supports in writing this review. We would also like to dedicate this article to the Institute of Materials Science on the occasion of the 30th anniversary of its foundation.

CRediT authorship contribution statement. Nguyen Xuan Phuc - preparation of first manuscript draft, Do Hung Manh - scientific revision, Pham Hong Nam - collection of references and figure and tables preparation.

Declaration of competing interest. There are no conflicts to declare.

REFERENCES

1. Hossan M. R., and Dutta P. - Effects of temperature dependent properties in electromagnetic heating, J. Heat and Mass Transfer. **55** (2012) 3412-3422.
2. Habash R. W. Y., Bansal R., Krewski D., and Alhafid H. T. - Thermal therapy, part 1: an introduction to thermal therapy, Crit. Rev. Biomed. Eng. **34** (6) (2006) 459-489.
3. Bayerl T., Duhovic M., Mitschang P., and Bhattacharyya D. - The heating of polymer composites by electromagnetic induction - A review, Compos. A: Appl. Sci. Manuf. **57** (2014) 27-40.
4. Vashisth A., Upama S. T., Anas M., Oh J.-H., Patil N., and Green M. J. - Radio frequency heating and material processing using carbon susceptors, Nanoscale Adv. **3** (2021) 5255-5264.
5. Fink B. K., Yarlagadda S., Xiao J. Q., Laverty G. H., and Gillespie Jr J. W. - Functional Nanostructures for Induction Heating: A Review of Literature and Recommendations for Research, Army Research Laboratory (2000) ARL-TR-2365.
6. Govorov A. O., and Richardson H. H. - Generating heat with metal nanoparticles, Nano Today. **2** (2007) 30-38.
7. Baffou G., and Quidant R. - Thermo-plasmonics: using metallic nanostructures as nano-sources of heat, Laser Photonics Rev. **7** (2013) 171-187.
8. Sharma S. K., Shrivastava N., Rossi F., and Thanh N. T. K. - Nanoparticles-based magnetic and photo induced hyperthermia for cancer treatment, Nano Today. **29** (2019) 100795.
9. Hedayatnasab Z., Abnisa F., and Daud W. M. A. W. - Review on magnetic nanoparticles for magnetic nanofluid hyperthermia application, Mater. Des. **123** (2017) 174-196.
10. Jauffred L., Samadi A., Klingberg H., Bendix P. M., and Oddershede L. B. - Plasmonic heating of nanostructures, Chem. Rev. **119** (2019) 8087-8130.
11. Jaque D., Maestro L. M., Del Rosal B., Haro-Gonzalez P., Benayas A., Plaza J. L., Rodriguez E. M., and Sole J. G. - Nanoparticles for photothermal therapies, Nanoscale. **6** (2014) 9494-9530.
12. Pankhurst Q. A., Thanh N. T. K., Jones S. K., and Dobson J. - Progress in applications of magnetic nanoparticles in biomedicine. J. Phys. D. **42** (2009) 224001(15).
13. Baffou G., Cichos F., and Quidant R. - Applications and challenges of thermoplasmonics, Nat. Mater. **19** (2020) 946-958.
14. Etheridge M. L., Xu Y., Rott L., Choi J., Glasmacher B., and Bischof J. C. - RF heating of magnetic nanoparticles improves the thawing of cryopreserved biomaterials, Technology. **2** (2014) 229-242.
15. Bello F., Sanvito S., Hess O., and Donegan J. F. - Shaping and storing magnetic data using pulsed plasmonic nanoheating and spin-transfer torque, ACS Photonics. **6** (2019) 1524-1532.
16. Rosensweig R. E. - Heating magnetic fluid with alternating magnetic field, J. Magn. Magn. Mater. **252** (2002) 370-374.
17. Hergt R., Dutz S., Müller R., and Zeisberger M. - Magnetic particle hyperthermia: nanoparticle magnetism and materials development for cancer therapy, J. Condens. Matter Phys. **18** (2006) S2919-S2934.
18. Suto M., Hirota Y., Mamiya H., Fujita A., Kasuya R., Tohji K., and Jeyadevan B. - Heat dissipation mechanism of magnetite nanoparticles in magnetic fluid hyperthermia, J. Magn. Magn. Mater. **321** (2009) 1493-1496.

19. Deatsch A. E., and Evans B. A. - Heating efficiency in magnetic nanoparticle hyperthermia, J. Magn. Magn. Mater. **354** (2014) 163-172.
20. Phong P. T., Nguyen L. H., Lee I.-J., and Phuc N. X. - Computer simulations of contributions of Néel and Brown relaxation to specific loss power of magnetic fluids in hyperthermia, J. Electron. Mater. **46** (2017) 2393-2405.
21. Fink B. K., McCullough R. L., and Gillespie Jr J. W. - A local theory of heating in cross-ply carbon fiber thermoplastic composites by magnetic induction, Polymer Eng. & Science. **32** (1992) 357-369.
22. Vazquez E., and Prato M. - Carbon nanotubes and microwaves: interactions, responses, and applications, ACS nano. **3** (2009) 3819-3824.
23. Anas M., Zhao Y., Saed M. A., Ziegler K. J., and Green M. J. - Radio frequency heating of metallic and semiconducting single-walled carbon nanotubes, Nanoscale. **11** (2019) 9617-9625.
24. Gerringer J. C., Moran A. G., Habib T., Pospisil M. J., Oh J. H., Teipel B. R., and Green M. J. - Radio frequency heating of laser-induced graphene on polymer surfaces for rapid welding, ACS Appl. Nano Mater. **2** (2019) 7032-7042.
25. Hicks V. K., Anas M., Porter E. B., and Green M. J. - High-throughput screening of printed carbon nanotube circuits using radio frequency heating, Carbon. **152** (2019) 444-450.
26. Vashisth A., Healey R. E., Pospisil M. J., Oh J. H., and Green M. J. - Continuous processing of pre-pregs using radio frequency heating, Compos. Sci. Technol. **195** (2020) 108211.
27. Linh P. H., Van Thach P., Tuan N. A., Thuan N. C., and Phuc N. X. - Magnetic fluid based on Fe_3O_4 nanoparticles: Preparation and hyperthermia application, Journal of Physics, Conference Series, IOP Publishing **187** (2009) 1-5.
28. Fortin J. P., Wilhelm C., Servais J., Ménager C., Bacri J. C., and Gazeau F. - Size-sorted anionic iron oxide nanomagnets as colloidal mediators for magnetic hyperthermia, J. Am. Chem. Soc. **129** (2007) 2628-2635.
29. Lavorato G. C., Das R., Masa J. A., Phan M.-H., and Srikanth H. - Hybrid magnetic nanoparticles as efficient nanoheaters in biomedical applications, Nanoscale Adv. **3** (2021) 867-888.
30. Gneveckow U., Jordan A., Scholz R., Brüß V., Waldöfner N., Ricke J., Feussner A., Hildebrandt B., Rau B., and Wust P. - Description and characterization of the novel hyperthermia-and thermoablation-system for clinical magnetic fluid hyperthermia, Med. phys. **31** (2004) 1444-1451.
31. Sweeney C. B., Moran A. G., Gruener J. T., Strasser A. M., Pospisil M. J., Saed M. A., and Green M. J. - Radio frequency heating of carbon nanotube composite materials, ACS Appl. Mat. Interfaces. **10** (2018) 27252-27259.
32. Gonzales-Weimuller M., Zeisberger M., and Krishnan K. M. - Size-dependant heating rates of iron oxide nanoparticles for magnetic fluid hyperthermia, J. Magn. Magn. Mater. **321** (2009) 1947-1950.
33. Gonzalez-Fernandez M. A., Torres T. E., Andrés-Vergés M., Costo R., De la Presa P., Serna C. J., Morales M. P., Marquina C., Ibarra M. R., and Goya G. F. - Magnetic nanoparticles for power absorption: Optimizing size, shape and magnetic properties, J. Solid State Chem. **182** (2009) 2779-2784.
34. Gavilán H., Brollo M. E. F., Gutiérrez L., Veintemillas-Verdaguer S., and del Puerto Morales M. - Clinical Applications of Magnetic Nanoparticles In: Controlling the size and shape of

uniform magnetic iron oxide nanoparticles for biomedical applications by Thanh N. T. K., CRC Press, New York, USA, 2018.

35. Khurshid H., Alonso J., Nemati Z., Phan M. H., Mukherjee P., Fdez-Gubieda M. L., Barandiarán J. M., and Srikanth H. - Anisotropy effects in magnetic hyperthermia: A comparison between spherical and cubic exchange-coupled FeO/Fe_3O_4 nanoparticles, J. Appl. Phys. **117** (2015) 17A337.
36. (a) Lee J. H., Jang J. T., Choi J. S., Moon S. H., Noh S. H., Kim J. W., Kim J. G., Kim I. S., Park K. I., and Cheon J. - Exchange-coupled magnetic nanoparticles for efficient heat induction. Nat. Nanotechnol. **6** (2011) 418-422; (b) Noh S. H., Na W., Jang J. H., Lee J. H., Lee E. J., Moon S. H., Lim Y., Shin J. S., and Cheon J. - Nanoscale magnetism control via surface and exchange anisotropy for optimized ferrimagnetic hysteresis, Nano Lett. **12** (2012) 3716-3721.
37. Martinez-Boubeta C., Simeonidis K., Makridis A., Angelakeris M., Iglesias O., Guardia P., Cabot A., Yedra L., Estradé S., and Peiró F. - Learning from nature to improve the heat generation of iron-oxide nanoparticles for magnetic hyperthermia applications. Sci. Rep. **3** (2013) 1-8.
38. Yang M. D., Ho C. H., Ruta S., Chantrell R., Krycka K., Hovorka O., Chen F. R., Lai P. S., and Lai C. H. - Magnetic interaction of multifunctional core-shell nanoparticles for highly effective theranostics, Adv. Mater. **30** (2018) 1802444.
39. Mohapatra J., Xing M., Beatty J., Elkins J., Seda T., Mishra S. R., and Liu J. P. - Enhancing the magnetic and inductive heating properties of Fe_3O_4 nanoparticles via morphology control, Nanotechnology. **31** (2020) 275706.
40. Guardia P., Corato R. D., Lartigue L., Wilhelm C., Espinosa A., Garcia-Hernandez M., Gazeau F., Manna L., and Pellegrino T. - Water-soluble iron oxide nanocubes with high values of specific absorption rate for cancer cell hyperthermia treatment, ACS Nano. **6** (2012) 3080-3091.
41. Hugounenq P., Levy M., Alloyeau D., Lartigue L., Dubois E., Cabuil V. r., Ricolleau C., Roux S., Wilhelm C., and Gazeau F. - Iron oxide monocrystalline nanoflowers for highly efficient magnetic hyperthermia, J. Phys. Chem. C **116** (2012) 15702-15712.
42. Dutz S., Hergt R., Mürbe J., Müller R., Zeisberger M., Andrä W., Töpfer J., and Bellemann M. E. - Hysteresis losses of magnetic nanoparticle powders in the single domain size range, J. Magn. Magn. Mater. **308** (2007) 305-312.
43. Blanco-Andujar C., Ortega D., Southern P., Pankhurst Q., and Thanh N. - High performance multi-core iron oxide nanoparticles for magnetic hyperthermia: microwave synthesis, and the role of core-to-core interactions, Nanoscale. **7** (2015) 1768-1775.
44. Brezovich I. A. - Low frequency hyperthermia: capacitive and ferromagnetic thermoseed methods, Med. Phys. Monogr. **16** (1988) 82-111.
45. Hergt R., and Dutz S. - Magnetic particle hyperthermia—biophysical limitations of a visionary tumour therapy, J. Magn. Magn. Mater. **311** (2007) 187-192.
46. Herrero de la Parte B., Rodrigo I., Gutiérrez-Basoa J., Iturrizaga Correcher S., Mar Medina C., Echevarría-Uraga J. J., Garcia J. A., Plazaola F., and García-Alonso I. - Proposal of New Safety Limits for In Vivo Experiments of Magnetic Hyperthermia Antitumor Therapy, Cancers. **14** (2022) 3084.
47. Jain P. K., Huang X., El-Sayed I. H., and El-Sayed M. A. - Noble metals on the nanoscale: optical and photothermal properties and some applications in imaging, sensing, biology, and medicine, Acc. of Chem. Res. **41** (2008) 1578-1586.

48. (a) Link S., and El-Sayed M. A. - Shape and size dependence of radiative, non-radiative and photothermal properties of gold nanocrystals. Int. Rev. Phys. Chem. **19** (2000) 409-453; (b) Link S. and El-Sayed M.A. - Size and temperature dependence of the plasmon absorption of colloidal gold nanoparticles, J. Phys. Chem. B. **103** (1999) 4212.
49. Rocha U., Kumar K. U., Jacinto C., Villa I., Sanz-Rodríguez F., del Carmen Iglesias de la Cruz M., Juarranz A., Carrasco E., van Veggel F. C., and Bovero E. - Neodymium-Doped LaF3 Nanoparticles for Fluorescence Bioimaging in the Second Biological Window, Small. **10** (2014) 1141-1154.
50. Cheng L., Yang K., Chen Q., and Liu Z. - Organic stealth nanoparticles for highly effective in vivo near-infrared photothermal therapy of cancer, ACS nano. **6** (2012) 5605-5613.
51. Maestro L. M., Haro-González P., Sánchez-Iglesias A., Liz-Marzán L. M., Garcia Sole J., and Jaque D. - Quantum dot thermometry evaluation of geometry dependent heating efficiency in gold nanoparticles, Langmuir. **30** (2014) 1650-1658.
52. (a) Maestro L. M., Haro-Gonzalez P., del Rosal B., Ramiro J., Caamano A. J., Carrasco E., Juarranz A., Sanz-Rodriguez F., Sole J. G., and Jaque D. - Heating efficiency of multi-walled carbon nanotubes in the first and second biological windows, Nanoscale. **203** (5) (2013) 7882-7889; (b) Robinson J. T., Tabakman S. M., Liang Y., Wang H., Sanchez Casalongue H., Vinh D., and Dai H. - Ultrasmall reduced graphene oxide with high near-infrared absorbance for photothermal therapy, J. Am. Chem. Soc. **133** (2011) 6825-6831.
53. Hessel C. M., Pattani V. P., Rasch M., Panthani M. G., Koo B., Tunnell J. W., and Korgel B. A. - Copper Selenide Nanocrystals for Photothermal Therapy, Nano Lett. **11** (2011) 2560-2566.
54. Wawrzynczyk D., Bednarkiewicz A., Nyk M., Strek W., and Samoc M. - Neodymium (III) doped fluoride nanoparticles as non-contact optical temperature sensors, Nanoscale. **4** (2012) 6959-6961.
55. Tikhomirov V. K., Driesen K., Rodriguez V. D., Gredin P., Mortier M., and Moshchalkov V. V. - Optical nanoheater based on the Yb^{3+}-Er^{3+} co-doped nanoparticles, Opt. Express. **17** (2009) 11794-11798.
56. Espinosa A., Bugnet M., Radtke G., Neveu S., Botton G. A., Wilhelm C., and Abou-Hassan A. - Can magneto-plasmonic nanohybrids efficiently combine photothermia with magnetic hyperthermia?, Nanoscale. **7** (2015) 18872-18877.
57. Di Corato R., Béalle G., Kolosnjaj-Tabi J., Espinosa A., Clement O., Silva A. K. A., Menager C., and Wilhelm C. - Combining magnetic hyperthermia and photodynamic therapy for tumor ablation with photoresponsive magnetic liposomes, ACS Nano. **9** (2015) 2904-2916.
58. Fang W., Zhang H., Wang X., Wei W., Shen Y., Yu J., Liang J., Zheng J., and Shen Y. - Facile synthesis of tunable plasmonic silver core/magnetic Fe_3O_4 shell nanoparticles for rapid capture and effective photothermal ablation of bacterial pathogens, New J. Chem. **41** (2017) 10155-10164.
59. Zhang H., Yang Z., Ju Y., Chu X., Ding Y., Huang X., Zhu K., Tang T., Su X., and Hou Y. - Galvanic Displacement Synthesis of Monodisperse Janus-and Satellite-Like Plasmonic–Magnetic Ag–Fe@ Fe3O4 Heterostructures with Reduced Cytotoxicity, Adv. Sci. **5** (2018) 1800271(9).
60. Wang D., Wang K., and Xu W. - Novel fabrication of magnetic thermoplastic nanofibers via melt extrusion of immiscible blends, Polym. Adv. Technol. **24** (2013) 70-74.

61. Milad M. M. M., Ahmad S. H., Yahya S. Y., and Tarawneh M. a. A. - Mechanical and Magnetic Properties of Thermoplastic Natural Rubber Nanocomposites Filled with Barium Ferrit, AIP Conference Proceedings **1136** (2009) 46-50.
62. Vasudevan M. P., Sudeep P. M., Al-Omari I. A., Kurian P., Ajayan P. M., Narayanan T. N., and Anantharaman M. R. - Enhanced microactuation with magnetic field curing of magnetorheological elastomers based on iron–natural rubber nanocomposites, Bull. Mater. Sci. **38** (2015) 689-694.
63. Herren B., Charara M., Saha M. C., Altan M. C., and Liu Y. - Rapid Microwave Polymerization of Porous Nanocomposites with Piezoresistive Sensing Function, Nanomaterials. **10** (2020) 233.
64. Sweeney C. B., Lackey B. A., Pospisil M. J., Achee T. C., Hicks V. K., Moran A. G., Teipel B. R., Saed M. A., and Green M. J. - Welding of 3D-printed carbon nanotube-polymer composites by locally induced microwave heating, Sci. Adv. **3** (2017) e1700262.
65. Anas M., Mustafa M. M., Vashisth A., Barnes E., Saed M. A., Moores L. C., and Green M. J. - Universal patterns of radio-frequency heating in nanomaterial-loaded structures, Appl. Mat. Today. **23** (2021) 101044.
66. Gilchrist R. K., Medal R., Shorey W. D., Hanselman R. C., Parrott J. C., and Taylor C. B. - Selective inductive heating of lymph nodes, Ann. Surg. **146** (1957) 596-606.
67. Jordan A., Wust P., Fähling H., John W., Hinz A., and Felix R. - Inductive heating of ferrimagnetic particles and magnetic fluids: Physical evaluation of their potential for hyperthermia, Int. J. Hyperth. **9** (1993) 51-68.
68. Hilger I. - In vivo applications of magnetic nanoparticle hyperthermia, Int. J. Hyperth. **29** (2013) 828-834.
69. Sadhukha T., Lin Niu, Wiedmann T.S., and Panyam J. - Effective elimination of cancer stem cells by magnetic hyperthermia, Molecular pharmaceutics. **10** (4) (2013) 1432-1441.
70. Sadhukha T., Wiedmann T. S., and Panyam J. - Inhalable magnetic nanoparticles for targeted hyperthermia in lung cancer therapy, Biomaterials. **34** (21) (2013) 5163-5171.
71. Hoopes P. J., Strawbridge R. R., Gibson U. J., Zeng Q., Pierce Z. E., Savellano M., Tate J. A., Ogden J.A., and Baker I. - Intratumoral iron oxide nanoparticle hyperthermia and radiation cancer treatment, In Thermal Treatment of Tissue: Energy Delivery and Assessment IV, Vol. 6440, pp. 174-183. SPIE, 2007. doi:10.1117/2.706302.
72. Lin M., Huang J., and Sha M. - Recent advances in nanosized Mn–Zn ferrite magnetic fluid hyperthermia for cancer treatment, J. Nanosci. Nanotechnol. **14** (2014) 792-802.
73. Rodrigues H. F., Capistrano G., and Bakuzis A. F. - *In vivo* magnetic nanoparticle hyperthermia: a review on preclinical studies, low-field nano-heaters, noninvasive thermometry and computer simulations for treatment planning, Int. J. Hyperth. **37** (2020) 76-99.
74. Thiesen B., and Jordan A. - Clinical applications of magnetic nanoparticles for hyperthermia, Int. J. Hyperth. **24** (2008) 467-474.
75. Luengo Y., Díaz-Riascos Z. V., García-Soriano D., Teran F. J., Artés-Ibáñez E. J., Ibarrola O., Somoza Á., Miranda R., Schwartz S., Abasolo I., and Salas G. - Fine Control of In Vivo Magnetic Hyperthermia Using Iron Oxide Nanoparticles with Different Coatings and Degree of Aggregation, Pharmaceutics. **14** (2022) 1526.
76. Pitsillides C. M., Joe E. K., Wei X., Anderson R. R., and Lin C. P. - Selective cell targeting with light-absorbing microparticles and nanoparticles, Biophys. J. **84** (2003) 4023-4032.

77. Hirsch L. R., Stafford R. J., Bankson J. A., Sershen S. R., Rivera B., Price R. E., Hazle J. D., Halas N. J., and West J. L. - Nanoshell-mediated near-infrared thermal therapy of tumors under magnetic resonance guidance, Proc. Natl. Acad. Sci. **100** (2003) 13549-13554.

78. Ali M. R. K., Ibrahim I. M., Ali H. R., Selim S. A., and El-Sayed M. A. - Treatment of natural mammary gland tumors in canines and felines using gold nanorods-assisted plasmonic photothermal therapy to induce tumor apoptosis, Int. J. Nanomed. **11** (2016) 4849.

79. Nomura S., Morimoto Y., Tsujimoto H., Arake M., Harada M., Saitoh D., Hara I., Ozeki E., Satoh A., Takayama E., Hase K., Kishi Y., and Ueno H. - Highly reliable, targeted photothermal cancer therapy combined with thermal dosimetry using a near-infrared absorbent, Sci. Rep. **10** (2020) 9765.

80. Han H. S., and Choi K. Y. - Advances in Nanomaterial-Mediated Photothermal Cancer Therapies: Toward Clinical Applications, Biomedicines. **9** (2021) 305.

81. Zhao L., Zhang X., Wang X., Guan X., Zhang W., and Ma J. - Recent advances in selective photothermal therapy of tumor, J. Nanotechnol. **19** (2021) 335.

82. Sun J., Zhao H., Xu W., and Jiang G.-Q. - Recent advances in photothermal therapy-based multifunctional nanoplatforms for breast cancer, Front. Chem. **10** (2022) 1024177.

83. Gannon C. J., Cherukuri P., Yakobson B. I., Cognet L., Kanzius J. S., Kittrell C., Weisman R. B., Pasquali M., Schmidt H. K., Smalley R. E., and Curley S. A. - Carbon nanotube-enhanced thermal destruction of cancer cells in a noninvasive radiofrequency field, Cancer. **110** (2007) 2654-2665.

84. Derfus A. M., von Maltzahn G., Harris T. J., Duza T., Vecchio K. S., Ruoslahti E., and Bhatia S. N. - Remotely Triggered Release from Magnetic Nanoparticles, Adv. Mater. **19** (2007) 3932-3936.

85. Brazel C. S. - Magnetothermally-responsive Nanomaterials: Combining Magnetic Nanostructures and Thermally-Sensitive Polymers for Triggered Drug Release, Phar. Res. **26** (2009) 644-656.

86. Kumar C. S. S. R., and Mohammad F. - Magnetic nanomaterials for hyperthermia-based therapy and controlled drug delivery, Adv. Drug Deliv. Rev. **63** (2011) 789-808.

87. Stanley S. A., Gagner J. E., Damanpour S., Yoshida M., Dordick J. S., and Friedman J. M. - Radio-Wave Heating of Iron Oxide Nanoparticles Can Regulate Plasma Glucose in Mice, Sci. **336** (2012) 604-608.

88. Moros M., Idiago-López J., Asín L., Moreno-Antolín E., Beola L., Grazú V., Fratila R. M., Gutiérrez L., and de la Fuente J. M. - Triggering antitumoural drug release and gene expression by magnetic hyperthermia, Adv. Drug Deliv. Rev. **138** (2019) 326-343.

89. Thong P. Q., Huong L. T., Tu N. D., Nhung H.T.M., Khanh L., Manh D. H., Nam P. H., Phuc N. X., Alonso J., Qiao J., Sridhar S., Thu H. P., Phan M. H., Thanh N. T. K. - Multifunctional nanocarriers of Fe_3O_4@PLA-PEG/curcumin for MRI, magnetic hyperthermia and drug delivery, Nanomedicine. **17** (2023) 1677-1693.

90. Barhoumi A., Huschka R., Bardhan R., Knight M. W., and Halas N. J. - Light-induced release of DNA from plasmon-resonant nanoparticles: Towards light-controlled gene therapy, Chem. Phys. Lett. **482** (2009) 171-179.

91. Huschka R., Zuloaga J., Knight M. W., Brown L. V., Nordlander P., and Halas N. J. - Light-Induced Release of DNA from Gold Nanoparticles: Nanoshells and Nanorods, J. Am. Chem. Soc. **133** (2011) 12247-12255.

92. Andersen T., Bahadori A., Ott D., Kyrsting A., Reihani S. N. S., and Bendix P. M. - Nanoscale phase behavior on flat and curved membranes, Nanotechnology. **25** (2014) 505101.
93. Urban P., Kirchner S. R., Mühlbauer C., Lohmüller T., and Feldmann J. - Reversible control of current across lipid membranes by local heating, Sci. Rep. **6** (2016) 22686.
94. Hernández Montoto A., Montes R., Samadi A., Gorbe M., Terrés J. M., Cao-Milán R., Aznar E., Ibañez J., Masot R., Marcos M. D., Orzáez M., Sancenón F., Oddershede L. B., and Martínez-Máñez R. - Gold Nanostars Coated with Mesoporous Silica Are Effective and Nontoxic Photothermal Agents Capable of Gate Keeping and Laser-Induced Drug Release, ACS Appl. Mater. Interface. **10** (2018) 27644-27656.
95. Evans S. - Electromagnetic rewarming: the effect of CPA concentration and radio source frequency on uniformity and efficiency of heating, Cryobiology. **40** (2000) 126-138.
96. Eisenberg D. P., Bischof J. C., and Rabin Y. - Thermomechanical stress in cryopreservation via vitrification with nanoparticle heating as a stress-moderating effect, J. Biomech. Eng. **138** (2016) 011010.
97. Manuchehrabadi N., Gao Z., Zhang J., Ring H. L., Shao Q., Liu F., McDermott M., Fok A., Rabin Y., Brockbank K. G. M., Garwood M., Haynes C. L., and Bischof J. C. - Improved tissue cryopreservation using inductive heating of magnetic nanoparticles, Sci. Transl. Med. **9** (2017) eaah4586.
98. Cao M., Xu Y., and Dong Y. - Improving Mechanical Properties of Vitrified Umbilical Arteries with Magnetic Warming, Fluid dynamics & Materials Processing. **17** (2021) 123-139.
99. Zhan T., Liu K., Yang J., Dang H., Chen L., and Xu Y. - Fe_3O_4 Nanoparticles with Carboxylic Acid Functionality for Improving the Structural Integrity of Whole Vitrified Rat Kidneys, ACS Appl. Nano Mat. **4** (2021) 13552-13561.
100. Sharma A., Rao J. S., Han Z., Gangwar L., Namsrai B., Gao Z., Ring H. L., Magnuson E., Etheridge M., Wowk B., Fahy G. M., Garwood M., Finger E. B., and Bischof J. C. - Vitrification and Nanowarming of Kidneys, Adv. Sci. **8** (2021) 2101691.
101. Yang Y., He J., Li Q., Gao L., Hu J., Zeng R., Qin J., Wang S. X., and Wang Q. - Self-healing of electrical damage in polymers using superparamagnetic nanoparticles, Nature Nanotech. **14** (2019) 151-155.
102. Habib T., Patil N., Zhao X., Prehn E., Anas M., Lutkenhaus J. L., Radovic M., and Green M. J. - Heating of $Ti_3C_2T_x$ MXene/polymer composites in response to Radio Frequency fields, Sci. Rep. **9** (2019) 16489.
103. Gruener J. T., Vashisth A., Pospisil M. J., Camacho A. C., Oh J.-H., Sophiea D., Mastroianni S. E., Auvil T. J., and Green M. J. - Local heating and curing of carbon nanocomposite adhesives using radio frequencies, Journal of Manufacturing Processes. **58** (2020) 436-442.
104. Vashisth A., Auvil T. J., Sophiea D., Mastroianni S. E., and Green M. J. - Using Radio-Frequency Fields for Local Heating and Curing of Adhesive for Bonding Metals, Adv. Eng. Mat. **23** (2021) 2100210.
105. Sosnowchik B. D., and Lin L.W. - Rapid synthesis of carbon nanotubes via inductive heating, Applied physics letters. **89** (19) (2006) 193112.
106. Niether C., Faure S., Bordet A., Deseure J., Chatenet M., Carrey J., Chaudret B., Rouet A. - Improved water electrolysis using magnetic heating of FeC-Ni core-shell nanoparticles, Nature Energy. **3** (2018) 476-483, DOI: 10.1038/ s41560-018-0132-1.
107. Kobayashi S., Kikukawa N., Sugasawa M., and Yamaura I. - Method for regenerating adsorbent by heating, US 2005/018406 A1 (2005).

108. Kikukawa N., Takemori M., Nagano Y., Sugasawa M., and Kobayashi S. - Synthesis and magnetic properties of nanostructured spinel ferrites using a glycine–nitrate process, J. Magn. Magn. Mater. **284** (2004) 206-214.

109. (a) Phuc N. X., Tuan N. A., Thuan N. C., Tuan V. A., and Hong L. V. - Magnetic nanoparticles as smart heating mediator for hyperthermia and sorbent reggeneration, Advanced Materials Research, Trans Tech. Publ. **55-57** (2008) 27-32; (b) Phuc N. X., Yen H., Linh B. H., Tuan N. A., Thuan N. C., Hong L. V., Thang D. C., Thanh H. V., T. P. D., and Tuan V. A. – Investigations of (Mn-Zn) spinel ferrite nanoparticles and application in VOC desorption by magnetic heating, Procds. International Workshop on Nanotechnology & Application, IWNA Vung Tau, Viet Nam 2007, pp. 232-235.

110. Lin L., Wang M., Peng X., Lissek E. N., Mao Z., Scarabelli L., Adkins E., Coskun S., Unalan H. E., Korgel B. A., Liz-Marzán L. M., Florin E.-L., and Zheng Y. - Opto-thermoelectric nanotweezers, Nat. Photonics. **12** (2018) 195-201.

111. Uchida K., Takahashi S., Harii K., Ieda J., Koshibae W., Ando K., Maekawa S., and Saitoh E. - Observation of the spin Seebeck effect, Nature. **455** (2008) 778-781.

112. Choi G. M., Min B. C., Lee K. J., and Cahill D. G. - Spin current generated by thermally driven ultrafast demagnetization, Nat. Commun. **5** (2014) 4334.

113. Bello F., Wolf D., Parker G. J., Wolf C., Krichevsky A., Zong F., Abadía N., and Donegan J. F. - Optical, thermal, and bit-writing analysis of a directly coupled plasmonic waveguide for heat-assisted magnetic recording, OSA Continuum. **3** (2020) 2010-2021.